An $\mathcal{O}(1)$ algorithm for the numerical evaluation of the Sturm-Liouville eigenvalues of the spheroidal wave functions of order zero

Rafeh Rehan[a], James Bremer[a,*]

[a]*Department of Mathematics, University of Toronto*

Abstract

In addition to being the eigenfunctions of the restricted Fourier operator, the angular spheroidal wave functions of the first kind of order zero and nonnegative integer characteristic exponents are the solutions of a singular self-adjoint Sturm-Liouville problem. The running time of the standard algorithm for the numerical evaluation of their Sturm-Liouville eigenvalues grows with both bandlimit and characteristic exponent. Here, we describe a new approach whose running time is bounded independent of these parameters. Although the Sturm-Liouville eigenvalues are of little interest themselves, our algorithm is a component of a fast scheme for the numerical evaluation of the prolate spheroidal wave functions developed by one of the authors. We illustrate the performance of our method with numerical experiments.

Keywords: fast algorithms, special functions, spheroidal wave functions, ordinary differential equations

1. Introduction

The angular prolate spheroidal wave functions of the first kind of order zero and nonnegative integer characteristic exponents

$$Ps_0(z;\gamma),\ Ps_1(z;\gamma),\ Ps_2(z;\gamma),\ \ldots \tag{1}$$

are the eigenfunctions of the restricted Fourier operator

$$\mathscr{F}_\gamma[f](z) = \int_{-1}^{1} \exp(i\gamma t z) f(t)\ dt. \tag{2}$$

As such they provide an efficient mechanism for representing functions in the image of $\mathscr{F}_\gamma$, which is the space of functions with bandlimit γ. Indeed, the magnitudes of the first $2/\pi\gamma$ eigenvalues of the restricted Fourier operator are close to $\sqrt{2\pi/\gamma}$, the magnitudes of the next $\mathcal{O}(\log(\gamma))$ eigenvalues decay extremely rapidly, and the remaining eigenvalues are all close to zero [11]. It follows that only the first $2/\pi\gamma + \mathcal{O}(\log(\gamma))$ functions in (1) are needed to represent elements of the image of $\mathscr{F}_\gamma$ with high relative accuracy.

The behaviour of the spectrum of the restricted Fourier operator makes the numerical calculation of $Ps_n(z;\gamma)$ and the corresponding eigenvalue $\lambda_n(\gamma)$ through the direct discretization of (2) extremely difficult. Fortunately, the functions (1) are also the solutions of the singular self-adjoint Sturm-

*Corresponding author

Email address: bremer@math.toronto.edu (James Bremer)

Liouville problem

$$\begin{cases} (1-z^2)y''(z) - 2zy'(z) + (\chi - \gamma^2 z^2)y(z) = 0, \quad -1 < z < 1, \\ \lim\limits_{z \to \pm 1} y'(z)\sqrt{1-z^2} = 0 \end{cases} \tag{3}$$

(see, for instance, Section 3.8 of [12]). We refer to the differential equation in (3) as the reduced spheroidal wave equation because it is obtained from the more familiar spheroidal wave equation by deleting one of its parameters (order).

The Osipov-Xiao-Rokhlin method [21, 14], which is the standard approach to the numerical calculation of $Ps_n(z;\gamma)$ and the corresponding Sturm-Liouville eigenvalue $\chi_n(\gamma)$, operates by representing a solution of (3) as a finite Legendre expansion. While the dependence of its running time on the parameters γ and n is not fully understood, the numerical experiments of [16] suggest that it grows as $\mathcal{O}\left(n + \sqrt{n\gamma}\right)$, at least for large values of n and γ.

In [2], a numerical scheme for calculating $Ps_n(z;\gamma)$ which runs in time independent of n and which grows sublogarithmically with γ is described. However, it requires knowledge of the value of $\chi_n(\gamma)$. Here, we describe a mechanism for evaluating $\chi_n(\gamma)$ with near machine precision accuracy in time independent of γ and n. It proceeds by constructing a piecewise polynomial expansion of a nonstandard analytic continuation $\chi_\xi(\gamma)$ of $\chi_n(\gamma)$. The parameter ξ is related to the value of a certain phase function for the reduced spheroidal wave equation at the point 0, and we also construct expansions which allow for the rapid evaluation of the values of the first few derivatives of this phase function at 0. The ability to rapidly evaluate these quantities allows us to accelerate the algorithm of [2], reducing its running time by a factor of 10 or so.

Many second order differential equations admit phase functions which are easier to represent using standard mechanisms (such as polynomial expansions) than the solutions of the equations themselves. This is often demonstrated by proving that the equation admits a modulus function which satisfies various monotonicity properties. It is well known that Legendre's differential equation, which is a special case of the reduced spheroidal wave equation, possesses such a modulus function (see, for instance, [3]). Here, we conjecture that the reduced spheroidal wave equation admits a modulus function with properties similar to this modulus function for Legendre's differential equation. We also present the results of numerical experiments showing that, in any case, $\chi_\xi(\gamma)$ can be represented extremely efficiently via polynomial expansions. Indeed, the expansion of $\chi_\xi(\gamma)$ we constructed for this article consumes less than 0.76 MB of memory and allows for evaluation of $\chi_n(\gamma)$ for all $2^6 \leqslant \gamma \leqslant 2^{20}$ and $0 \leqslant n \leqslant 1.1\gamma$. Each evaluation takes less than 5×10^{-6} seconds on the standard desktop computer used to conduct the experiments of this paper. The range $0 \leqslant n \leqslant 1.1\gamma$ was chosen because

$$\lambda_{\lfloor 1.1\gamma \rfloor}(\gamma) < \epsilon_0 \tag{4}$$

for all $\gamma \geqslant 2^6 = 64$, where $\epsilon_0 = 2^{-52} \approx 2.220446049250313 \times 10^{-16}$ is machine zero for IEEE double precision arithmetic. The Osipov-Xiao-Rokhlin algorithm is more efficient than the approach suggested here for values of γ smaller than 64, and it is to be preferred in that regime. However, expansions which hold for a larger range of the parameters, including smaller values of γ, could easily be constructed.

The properties of $\chi_\xi(\gamma)$ are in stark contrast to those of the standard analytic continuation $\chi_\nu(\gamma)$ of $\chi_n(\gamma)$ obtained via characteristic exponents (see, for instance, [12]). The latter is entire in γ, but only meromorphic in ν, with branch points at each half-integer value of ν. This greatly complicates any attempt to construct expansions of $\chi_\nu(\gamma)$ using standard machinery, like polynomial

or trigonometric expansions.

The remainder of this article is structured as follows. Section 2 briefly discusses phase functions for second order linear ordinary differential equations. In Section 3, we define certain standard solutions of the reduced spheroidal wave equation and a define a particular phase function for the reduced spheroidal wave equation which plays a central role in our algorithm. Section 3 includes a discussion of characteristic exponents and the standard analytic continuations of $\chi_n(\gamma)$ and the spheroidal wave functions. In Section 4, we give several conjectures regarding the properties of a particular phase function for the reduced spheroidal wave equation and discuss some consequences of these conjectures. In Section 5, we introduce an alternative to characteristic exponents for indexing the reduced spheroidal wave functions. Section 6 details our numerical algorithm. In Section 7, we present the results of numerical experiments demonstrating the properties of our algorithm.

2. Phase functions for second order differential equations

Suppose that Ω is a simply-connected open set in the complex plane, and that $q : \Omega \to \mathbb{C}$ is an analytic function. Then we say that $\psi : \Omega \to \mathbb{C}$ is a phase function for the second order linear ordinary differential equation

$$y''(z) + q(z)y(z) = 0, \quad z \in \Omega, \tag{5}$$

provided ψ' does not vanish on Ω and

$$u(z) = \frac{\sin(\psi(z))}{\sqrt{\psi'(z)}} \quad \text{and} \quad v(z) = \frac{\cos(\psi(z))}{\sqrt{\psi'(z)}} \tag{6}$$

form a basis in the space of solutions of (5). The particular realization of the square root used in (6) is immaterial. It can be verified through a straightforward calculation that ψ' satisfies the second order nonlinear ordinary differential equation

$$q(z) - (\psi'(z))^2 + \frac{3}{4}\left(\frac{\psi''(z)}{\psi'(z)}\right)^2 - \frac{1}{2}\frac{\psi'''(z)}{\psi'(z)} = 0, \tag{7}$$

which we call Kummer's equation after E.E. Kummer who studied it in [10]. Conversely, if ψ' does not vanish in Ω and satisfies (7) then the function u and v defined via (6) are solutions of (5). In light of (6), we refer to

$$m(z) = \frac{1}{\psi'(z)} = (u(z))^2 + (v(z))^2 \tag{8}$$

as the modulus function associated with the phase function ψ'.

If u, v is a pair of solutions of (5) whose (necessarily constant) Wronskian w is nonzero on Ω and such that the modulus function (8) does not vanish on Ω, then it can be easily verified that the function

$$\psi'(z) = \frac{w}{(u(z))^2 + (v(z))^2} \tag{9}$$

satisfies Kummer's equation. It follows that any antiderivative ψ of ψ' is a phase function for (5). Adding the requirement that (6) holds determines ψ up to an additive constant multiple of 2π.

3. The prolate spheroidal wave functions of order zero

In this section, we discuss characteristic exponents, review the definitions of some of the standard solutions of the spheroidal wave function and define a certain phase function for the reduced

spheroidal wave equation.

3.1. The spheroidal wave equation

The spheroidal wave equation

$$(1-z^2)y''(z) - 2zy'(z) + \left(\chi - \gamma^2 z^2 - \frac{\mu^2}{1-z^2}\right) y(z) = 0 \tag{10}$$

arises when the method of separation of variables is used to solve the constant coefficient Helmholtz equation (see, for instance, Chapter 5 of [13]). When $\gamma^2 > 0$, its solutions are known as prolate spheroidal wave functions, and when $\gamma^2 < 0$ they are known as the oblate spheroidal wave functions. The spheroidal wave functions are typically indexed via the explicit parameters γ and μ, which we refer to as the bandlimit and order, respectively, and by an implicit parameter ν known as the characteristic exponent. The explicit parameter χ in (10) is usually regarded as a function of γ, μ and ν.

In this article, we restrict our attention to the prolate spheroidal wave functions of order zero (i.e., we impose the restrictions $\gamma^2 > 0$ and $\mu = 0$). These are the spheroidal wave functions which are the most widely used in applications. Obviously, they are solutions of the differential equation

$$(1-z^2)y''(z) - 2zy'(z) + \left(\chi - \gamma^2 z^2\right) y(z) = 0, \tag{11}$$

which we call the reduced spheroidal wave equation. It has regular singular points at $z = \pm 1$ and an irregular singular point at infinity.

3.2. Characteristic exponents

For any complex value of the parameter χ, (11) admits a solution of the form

$$z^\nu \sum_{n=-\infty}^{\infty} a_n z^{2n} \tag{12}$$

with the Laurent expansion convergent in the annulus $1 < |z| < \infty$ and, in the event that ν is not a half-integer, there is a second solution of the form

$$z^{-\nu-1} \sum_{n=-\infty}^{\infty} b_n z^{2n}, \tag{13}$$

also with the Laurent expansion convergent in the annulus $1 < |z| < \infty$ (see, for instance, [9] or [7]). The parameter χ appearing in (11) obviously only determines the value of ν up to an integral multiple of 2. It is less obvious that for each value of ν which is not a half-integer, there are a countable collection of values of χ such that (11) admits a pair of solutions, one of which is of the form (12) and the other is of the form (13). A proof of this appears in [12].

It is standard (again, see [12]) to associate a unique value of χ, which we denote by $\chi_\nu(\gamma)$, with each ν which is not a half-integer by requiring that

$$\lim_{\gamma \to 0^+} \chi_\nu(\gamma) = \nu(\nu+1). \tag{14}$$

This condition is motivated by that fact that (11) reduces to Legendre's differential equation when $\gamma = 0$. In that case, there is a solution of the form

$$z^\nu \sum_{n=0}^{\infty} a_n z^{2n}, \tag{15}$$

where $a_0 \neq 0$, and it can be easily seen that χ relates to ν via the formula $\chi = \nu(\nu+1)$.

The function $\chi_\nu(\gamma)$ which results from imposing the condition (14) is analytic in γ, but only meromorphic in ν, with branch points at the half-integers. Figure 1, which contains a plot of $\chi_\nu(\gamma)$ as a function of ν when $\gamma = 2$, shows the jump discontinuities that occur at half-integer values of ν. Moreover, because $\nu(\nu+1) = (-\nu-1)(-\nu)$, we have that $\chi_\nu(\gamma) = \chi_{-\nu-1}(\gamma)$. However, since the value of χ determines the possible values of ν in (12) and (13) up to an additive constant which is an integral multiple of 2, these are the only two values of ν which can correspond to a particular choice of χ.

While it is not possible to extend this scheme in order to assign a unique value of χ to each half-integer value of ν, one can associate two distinct values of χ to each half-integer ν by taking limits from the left and right. Further information on the case of half-integer characteristic exponents can be found in [8]. In what follows, we will assume implicitly that ν is not a half-integer and this will cause no difficulties for us.

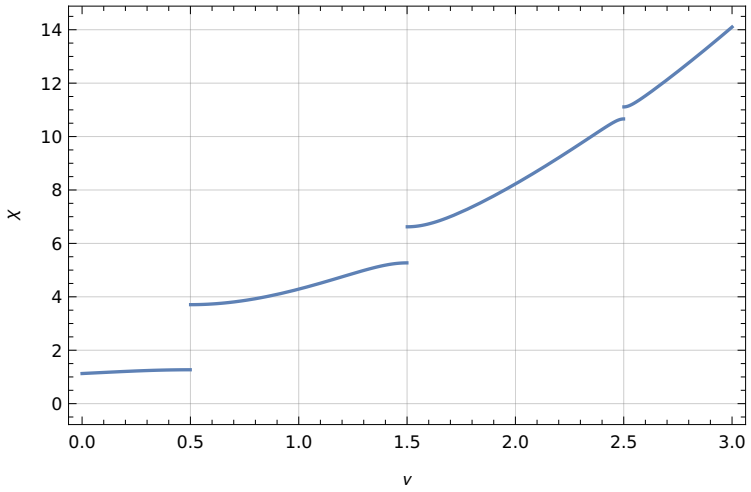

Figure 1: A plot of the standard analytic continuation $\chi_\nu(\gamma)$ of $\chi_n(\gamma)$ as a function of ν when $\gamma = 2$. There is a jump discontinuity at each half-integer value of ν.

3.3. The angular prolate spheroidal wave functions of the first and second kinds of order zero

Zero is a double root of the indicial equation for the reduced spheroidal wave equation corresponding to the regular singular point at $z = 1$. Accordingly, it admits a one-dimensional subspace of solutions which are regular at 1 and a one-dimensional subspace of solutions which have logarithmic singularities at 1 (see, for instance, [7]).

We use $Ps_\nu(z;\gamma)$ to denote the unique solution of (11) which is regular at $z = 1$ and such that either the value of $Ps_\nu(0;\gamma)$ agrees with that of the Legendre function $P_\nu(0)$ or, in the event that $P_\nu(0) = 0$, the derivative of $Ps_\nu(x;\gamma)$ with respect to x at 0 agrees with the derivative of the Legendre function $P_\nu(x)$ at 0. We refer to $Ps_\nu(z;\gamma)$ as the angular spheroidal wave function of the first kind of bandlimit γ, order zero and characteristic exponent ν. It is well known that $Ps_\nu(z;\gamma)$ admits an expansion of the form

$$Ps_\nu(z;\gamma) = \sum_{k=-\infty}^{\infty} a_k(\nu;\gamma) P_{\nu+2k}(z) \tag{16}$$

and, like the Legendre functions of the first kind, $Ps_\nu(z;\gamma)$ is entire as a function of z when ν is an integer and is single-valued on the cut-plane $\mathbb{C}\setminus(-\infty,-1]$ when ν is not an integer.

Assuming ν is not an integer, it can be easily verified that

$$Qs_\nu(z;\gamma) = \sum_{k=-\infty}^{\infty} a_k(\nu;\gamma) Q_{\nu+2k}(z), \tag{17}$$

where Q_ν is the Legendre function of the second kind of degree ν and the coefficients $\{a_k(\nu;\gamma)\}$ are the same as in (16), is also solution of the reduced spheroidal wave equation. The representation (17) is problematic when ν is an integer because $Q_\nu(z)$, when viewed as a function of ν, has simple poles at the negative integers. However, in this case, it is possible to find a representation of the form

$$Qs_\nu(z;\gamma) = \sum_{k=-\infty}^{\infty} b_k(\nu;\gamma) \frac{Q_{\nu+2k}(z)}{\Gamma(\nu+2k+1)} \tag{18}$$

since $\Gamma(\nu+1)$ has simple zeros at each negative integer (see, for instance, [12]). We refer to $Qs_\nu(z;\gamma)$ as the angular prolate spheroidal wave function of the second kind of bandlimit γ, order zero and characteristic exponent ν. Just like the Legendre functions of the second kind, the function $Qs_\nu(z;\gamma)$ is defined for z on the cut-plane $\mathbb{C}\setminus(-\infty,1]$ and has a logarithmic singularity at the point $z=1$.

Remark 1. *Some of the formulas in this article become simpler when $Ps_\nu(z,\gamma)$ is normalized through the requirement that $Ps_\nu(1,\gamma)=1$. This is in keeping with the standard convention for the normalization of the Legendre functions of the first kind. However, since many of the angular spheroidal wave functions decay exponentially on some portion of the interval $(0,1)$, such a normalization scheme would result in some of the $Ps_\nu(z,\gamma)$ taking on extremely large values in the interval $(0,1)$, thus complicating their numerical evaluation.*

3.4. The angular prolate spheroidal wave functions of the first kind of order zero and integer characteristic exponents

The boundary conditions

$$\lim_{z\to\pm1} y'(z)(1-z^2) = 0 \tag{19}$$

together with Equation (11) comprise a singular self-adjoint Sturm-Liouville problem (see, for example, [22] for a discussion of such problems.). The angular prolate spheroidal wave functions of the first kind of order zero and nonnegative integer characteristic exponents

$$Ps_0(z;\gamma),\ Ps_1(z;\gamma),\ Ps_2(z;\gamma),\ \ldots \tag{20}$$

are a collection of solutions of this Sturm-Liouville problem which form an orthogonal basis in $L^2(-1,1)$. Much of the interest in the spheroidal wave functions stems from the fact that (20) are also eigenfunctions of the restricted Fourier operator

$$\mathscr{F}_\gamma[f](z) = \int_{-1}^{1} \exp(i\gamma z t)\, f(t)\, dt. \tag{21}$$

This observation was widely publicized in the article [17] published in the 1960s, but it was known much earlier (see, for instance, Section 3.8 of [12] and the references cited there).

3.5. The radial prolate spheroidal wave functions of order zero

Another solution of (11), which is known as the radial spheroidal wave function of the third kind of order zero, is given by the formula

$$S_\nu^{(3)}(z;\gamma) = \frac{1}{Ps_\nu(1,\gamma)} \int_1^\infty \exp(i\gamma z t) Ps_\nu(t;\gamma)\, dt. \tag{22}$$

The integral is absolutely convergent for $\mathrm{Im}(z) > 0$ and $S_\nu^{(3)}(z;\gamma)$ is typically taken to be its analytic continuation to the cut plane $\mathbb{C}\backslash(-\infty, 1]$. However, it is more convenient for us to regard the domain of $S_\nu^{(3)}(z;\gamma)$ as the analytic continuation of (22) to an open simply-connected set Γ containing $\{z : \mathrm{Im}(z) \geqslant 0 \text{ and } z \neq \pm 1\}$. The asymptotic behaviour of $S_\nu^{(3)}(z;\gamma)$ can be easily deduced from (22):

$$S^{(3)}(z;\gamma) = \frac{\exp(i\gamma z)}{\gamma z} + \mathcal{O}\left(\frac{1}{z^2}\right) \quad \text{as} \quad z \to \infty. \tag{23}$$

Similarly, the radial prolate spheroidal wave function of the fourth kind of bandlimit γ, order zero and characteristic exponent ν is given by the formula

$$S_\nu^{(4)}(z;\gamma) = \frac{1}{Ps_\nu(1;\gamma)} \int_1^\infty \exp(-i\gamma z t) Ps_\nu(t;\gamma)\, dt. \tag{24}$$

The integral is absolutely convergent for $\mathrm{Im}(z) < 0$, and, like $S_\nu^{(3)}(z;\gamma)$, the domain of this function is usually taken to be the cut plane $\mathbb{C}\backslash(-\infty, 1]$. However, we regard $S_\nu^{(4)}(z;\gamma)$ as defined on the same open simply-connected set Γ which serves as the domain of $S_\nu^{(3)}(z;\gamma)$. It follows easily from (24) that

$$S^{(4)}(z;\gamma) = \frac{\exp(-i\gamma z)}{\gamma z} + \mathcal{O}\left(\frac{1}{z^2}\right) \quad \text{as} \quad z \to \infty. \tag{25}$$

We define the radial prolate spheroidal wave functions of the first and second kinds of bandlimit γ, order zero and characteristic exponent ν on Γ via the formulas

$$S_\nu^{(1)}(z;\gamma) = \frac{S_\nu^{(3)}(z;\gamma) + S_\nu^{(4)}(z;\gamma)}{2} \tag{26}$$

and

$$S_\nu^{(2)}(z;\gamma) = \frac{S_\nu^{(3)}(z;\gamma) - S_\nu^{(4)}(z;\gamma)}{2i}, \tag{27}$$

respectively. Then

$$S_\nu^{(3)}(z;\gamma) = S_\nu^{(1)}(z;\gamma) + iS_\nu^{(2)}(z;\gamma). \tag{28}$$

and

$$S_\nu^{(4)}(z;\gamma) = S_\nu^{(1)}(z;\gamma) - iS_\nu^{(2)}(z;\gamma). \tag{29}$$

Moreover, from (23) and (25) it easily follows that

$$S^{(1)}(z;\gamma) = \frac{\sin(\gamma z)}{\gamma z} + \mathcal{O}\left(\frac{1}{z^2}\right) \quad \text{as} \quad z \to \infty \tag{30}$$

and

$$S^{(2)}(z;\gamma) = \frac{\cos(\gamma z)}{\gamma z} + \mathcal{O}\left(\frac{1}{z^2}\right) \quad \text{as} \quad z \to \infty. \tag{31}$$

3.6. The normal form of the reduced spheroidal wave equation

A straightforward calculation shows that if y satisfies the reduced spheroidal wave equation (11), then the function $u(z) = y(z)\sqrt{1-z^2}$ satisfies

$$u''(z) + \left(\frac{1}{(1-z^2)^2} + \frac{\chi - \gamma^2 z^2}{1-z^2}\right) u(z) = 0, \quad z \in \Gamma. \tag{32}$$

The particular realization of $\sqrt{1-z^2}$ used here is immaterial. We refer to (32) as the normal form of the reduced spheroidal wave equation.

3.7. The phase and modulus functions associated with $S_\nu^{(3)}(z;\gamma)$

We define the functions $M_\nu(z;\gamma)$ and $\Psi S_\nu(z;\gamma)$ on Γ via the formulas

$$M_\nu(z;\gamma) = \left(S_\nu^{(1)}(z;\gamma)\right)^2 + \left(S_\nu^{(2)}(z;\gamma)\right)^2 \tag{33}$$

and

$$\Psi S_\nu(z;\gamma) = \int_1^z \frac{\gamma}{M_\nu(u;\gamma)(1-u^2)}\, du. \tag{34}$$

Since the Wronskian of any pair of solutions of the differential equation (32) is constant, it can be easily seen from (30) and (31) that the Wronskian of the pair $S_\nu^{(1)}(z;\gamma)\sqrt{1-z^2},\ S_\nu^{(2)}(z;\gamma)\sqrt{1-z^2}$ is γ. It follows that $\Psi S_\nu(z;\gamma)$ is a phase function for the normal form of the reduced spheroidal wave equation, and that $M_\nu(z;\gamma)(1-z^2)$ is the corresponding modulus function. We omit the factor of $(1-z^2)$ in the definition of $M_\nu(z;\gamma)$ to make stating the conjectures of Section 4 more convenient. Moreover, by a slight abuse of terminology, we will refer to $M_\nu(z;\gamma)$ as the modulus function associated with $\Psi S_\nu(z;\gamma)$.

Since $\Psi S_\nu(z;\gamma)$ is a phase function for (32), there exist $C_\nu(z;\gamma)$ and $D_\nu(z;\gamma)$ such that

$$Ps_\nu(z;\gamma)\sqrt{1-z^2} = C_\nu(z;\gamma)\frac{\sin\left(\Psi S_\nu(z;\gamma)\right)}{\sqrt{\frac{d\Psi S_\nu}{dz}(z,\gamma)}} + D_\nu(z;\gamma)\frac{\cos\left(\Psi S_\nu(z;\gamma)\right)}{\sqrt{\frac{d\Psi S_\nu}{dz}(z,\gamma)}}. \tag{35}$$

From (34), we see that (35) is equivalent to

$$Ps_\nu(z;\gamma) = C_\nu(z;\gamma)\frac{\sqrt{M_\nu(z;\gamma)}}{\sqrt{\gamma}}\sin\left(\Psi S_\nu(z;\gamma)\right) + D_\nu(z;\gamma)\frac{\sqrt{M_\nu(z;\gamma)}}{\sqrt{\gamma}}\cos\left(\Psi S_\nu(z;\gamma)\right). \tag{36}$$

Because $Qs_\nu(z;\gamma)$ has a logarithmic singularity at 1, we must have

$$\lim_{z\to 1}\left|\sqrt{M_\nu(z;\gamma)}\right| = \infty. \tag{37}$$

But we also have

$$\lim_{z\to 1}\Psi S_\nu(z;\gamma) = 0, \tag{38}$$

and it follows from this and (37) that

$$\lim_{z\to 1}\left|\sqrt{M_\nu(z;\gamma)}\cos\left(\Psi S_\nu(z;\gamma)\right)\right| = \infty. \tag{39}$$

Since $Ps_\nu(z;\gamma)$ is nonsingular at 1, we must have $D_\nu(\gamma) = 0$ in (35) and (36) so that

$$Ps_\nu(z;\gamma)\sqrt{1-z^2} = C_\nu(z;\gamma)\frac{\sin\left(\Psi S_\nu(z;\gamma)\right)}{\sqrt{\frac{d\Psi S_\nu}{dz}(z,\gamma)}}. \tag{40}$$

3.8. The reduced spheroidal wave functions as functions of the parameter χ

It follows easily both from mechanism used to define $Ps_\nu(z;\gamma)$ and from (16) that $Ps_{-\nu-1}(z;\gamma) = Ps_\nu(z;\gamma)$. In particular, $Ps_\nu(z;\gamma)$ is uniquely determined by the value of the parameter χ in (11). From this observation and the definitions of Section 3.5, it is clear that the radial spheroidal wave functions, and hence also $M_\nu(z;\gamma)$ and $\Psi S_\nu(z;\gamma)$, are uniquely determined by χ and hence can be indexed via χ instead of by ν. We note that it follows from (17) that this is not the case for $Qs_\nu(z;\gamma)$.

We will, by a slight abuse of notation, use $S_\chi^{(3)}(z;\gamma)$ to denote the radial spheroidal wave functions of the third kind corresponding to $\chi = \chi_\nu(\gamma)$, and likewise for $M_\chi(z;\gamma)$ and $\Psi S_\chi(z;\gamma)$. It follows from standard results in the theory of ordinary differential equations that these functions are entire in χ as well as in γ.

4. The monotonicity properties of the reduced spheroidal wave equation

It is well known that many second order differential equations admit modulus functions which satisfy strong monotonicity properties. Bessel's differential equation furnishes one such example. The formula

$$J_\lambda^2(z) + Y_\lambda^2(z) = \frac{2}{\pi}\int_0^\infty \exp(-zt) P_{\lambda-\frac{1}{2}}\left(1+\frac{t^2}{2}\right)\, dt, \tag{41}$$

which can be found in [6], expresses a modulus function for Bessel's equation as the Laplace transform of a positive function. Because of the close relationship between modulus and phase functions, it follows that Bessel's equation admits a phase functions which is, among other things, increasing and nonoscillatory on the interval $(0,\infty)$. This is in stark contrast to the Bessel functions themselves, which behave as increasing or decreasing exponential functions on the interval $\left(0,\sqrt{\lambda^2-1/4}\right)$ and oscillate on $\left(\sqrt{\lambda^2-1/4},\infty\right)$. The existence of this phase function was used at an early date to rapidly evaluate the Bessel functions [4] of large arguments, and it is exploited by the widely used algorithm [1] for the same purpose.

Similar results hold for many second order linear ordinary differential equations. Relevant formulas for the Jacobi functions, Gegenbauer functions and Hermite functions can be found in [3], and the articles [5] and [6] give conditions under which a second order linear ordinary differential equation admits a modulus function which is the Laplace transform of a nonnegative Borel measure.

The asymptotic estimates (23) and (25) indicates that, at least for large z, the modulus function $M_\nu(z;\gamma)$ can be well approximated by a nonoscillatory function. This suggests that $M_\nu(z;\gamma)$, like (41), satisfies various monotonicity properties. Our suspicions are further bolstered by the fact that Legendre's differential equation, which is a special case of (11), is known to satisfy certain strong monotonicity properties (see [3]). In this section, after briefly defining various notions of monotonicity, we make several conjectures about the monotonicity properties of $M_\nu(z;\gamma)$ and $S_\nu(z;\gamma)$. These conjectures were arrived at through numerical experiments, experiments using computer algebra systems and our belief that the properties of the reduced spheroidal wave equation are similar to those of Legendre's differential equation.

4.1. Monotonicity Properties

A smooth function f defined on an open interval I is completely monotone if $(-1)^j f^{(j)}(z) \geqslant 0$ for all nonnegative integers j and all $z \in I$. It is absolutely monotone provided provided $f^{(j)}(z) \geqslant 0$ for all nonnegative integers j and all $z \in I$. A k-times differentiable function f defined on an open interval I is k-times monotone provided $(-1)^j f^{(j)}(z) \geqslant 0$ for all nonnegative integers $j \leqslant k$ and all $z \in I$.

It is well known that f is completely monotone on $(0,\infty)$ if and only if f is the Laplace transform of a nonnegative Borel measure (see, for instance, [19]). Similarly, a function f is k-times monotone, where $k \geqslant 1$, on $(0,\infty)$ if and only if there is a nonnegative Borel measure α such that

$$f(x) = \int_0^{\frac{1}{x}} (1-tx)^{(k-1)}\, d\alpha(t). \tag{42}$$

Formula (42) suggests an obvious generalization of the notion of k-times monotone to noninteger values of k; that is, a function f is said to be ω-times monotone, where $\omega \geqslant 1$ is not necessarily an integer, provided there is a nonnegative Borel measure α such that

$$f(x) = \int_0^{\frac{1}{x}} (1 - tx)^{(\omega-1)} \, d\alpha(t). \tag{43}$$

See [20] for a proof of (42) and a discussion of the definition (43).

4.2. Conjectures regarding $S_\nu^{(3)}(z;\gamma)$, $M_\nu(z;\gamma)$ and $\Psi S_\nu(z;\gamma)$

We now state several conjectures regarding $S_\nu^{(3)}(z;\gamma)$ and the associated phase and modulus functions. The first of these asserts that the properties the modulus function $M_\nu(z;\gamma)$ mirror those of a modulus function for Legendre's differential equation.

Conjecture 1. *For fixed $\gamma > 0$ and $\nu > 0$, when viewed as a function of z, $M_\nu(z;\gamma)$ is absolutely monotone on $(0,1)$ and completely monotone on $(1,\infty)$.*

The second of our conjectures can be viewed as a stronger version of the Sturm Comparison Theorem in that it implies that the reduced spheroidal wave functions become more oscillatory as the parameter χ increases.

Conjecture 2. *For fixed $\gamma > 0$ and $-1 < z < 1$, $\Psi S_\chi(z;\gamma)$ is strictly decreasing on the interval $(0,\infty)$.*

Finally, we have following conjecture which generalizes one made in [2] to the case of noninteger values of ν:

Conjecture 3. *For a fixed $\gamma > 0$ and $\nu > 0$, when viewed as a function of z, $S_\nu^{(3)}(iz;\gamma)$ is $(\nu+2)$-times monotone on $(0,\infty)$.*

5. An alternative method for indexing the reduced spheroidal wave functions

Characteristic exponents are the standard mechanism for indexing the reduced spheroidal wave functions. This scheme has advantage that the solutions of most interest — those which are the eigenfunctions of the restricted Fourier operator — correspond to nonnegative integer characteristic exponents. However, it has the serious disadvantage that $\chi_\nu(\gamma)$ has branch points at the half-integer values of ν.

In Section 3.8, we observed that many of the spheroidal wave functions, as well as the phase and modulus functions defined in this article, can be indexed via the parameter χ appearing in the reduced spheroidal wave equation. It follows from standard results in the theory of ordinary differential equations that these functions are entire in both γ and χ. However, the values of χ corresponding to the nonnegative integer characteristic exponents are not apparent and require substantial effort to calculate.

We now discuss a new mechanism for indexing the reduced spheroidal wave functions which combines the advantages of both of these approaches. It is a consequence of (40) that the zeros of $Ps_\nu(z;\gamma)$ must occur at points z such that $\Psi S_\nu(z;\gamma)$ is an integral multiple of π. It is well known that when n is a nonnegative integer, $Ps_n(z;\gamma)$ has n zeros in the interval $[0,1)$, that it has a zero at the point $z = 0$ if n is odd, and that its first derivative has a zero at $z = 0$ if n is even (see, for instance, [12]). It follows from these observations that

$$\Psi S_n(0;\gamma) = -\frac{\pi}{2}\,(n+1) \tag{44}$$

whenever n is an nonnegative integer. Moreover, it is a consequence of Conjecture 2 that the map $\chi \to -\Psi S_\chi(0;\gamma)$ can be inverted. This suggests that we use the new parameter

$$\xi = -\frac{2}{\pi}\,\Psi S_\chi(0;\gamma) - 1 \tag{45}$$

to index the reduced spheroidal wave functions. From (44), we see that, just like characteristic exponents, nonnegative integer values of ξ correspond to the eigenfunctions of the restricted Fourier operator. Indeed, the parameter ξ generalizes the notion of "the number of zeros of the function $Ps_\nu(z;\gamma)$ on the interval $[0,1]$." Because the qualitative behaviour of the reduced spheroidal wave function $Ps_n(z;\gamma)$ is related to the ratio of the characteristic exponent n to γ, we find it slightly more convenient to use the parameter

$$\sigma = \frac{\xi}{\gamma}$$

to index χ and the spheroidal wave functions. We denote the value of χ corresponding to σ and γ by $\chi_\sigma(\gamma)$.

Figure 2 contains plots of $\chi_\sigma(\gamma)$ as a function of σ for several values of γ. We note that each of these graphs have inflection points when $\sigma \approx 2/\pi$. There is a regime change when σ is somewhat larger than $2/\pi$. For smaller values of σ, the reduced spheroidal wave equation has turning points in the interval $(0,1)$. But for larger values of σ, the spheroidal wave functions of order zero are oscillatory on the entire interval $(-1,1)$.

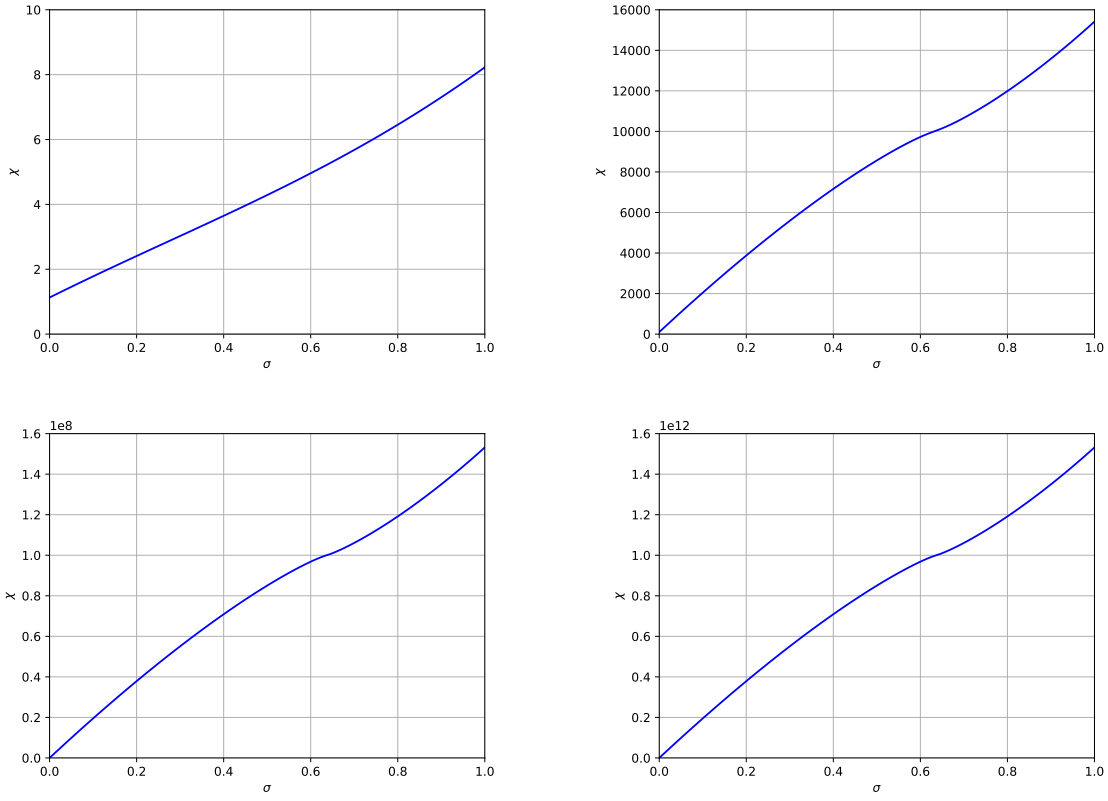

Figure 2: Plots of the parameter χ as a function of σ when $\gamma = 2$ (upper left), $\gamma = 100$ (upper right), $\gamma = 10,000$ (lower left) and when $\gamma = 10^6$ (lower right). The relationship between ξ and σ is $\xi = \gamma\sigma$.

6. Numerical algorithm

We now describe our method for the numerical evaluation of the Sturm-Liouville eigenvalues of the reduced spheroidal wave equation. In broad outline, it consists of precomputing a piecewise bivariate polynomial expansion of the function $\chi_\sigma(\gamma)$ which can then be used to rapidly evaluate $\chi_n(\gamma)$ for all $2^6 \leqslant \gamma \leqslant 2^{20}$ and all nonnegative integer values of n in the interval $[0, 1.1\gamma]$. For values of γ smaller than 2^6, the Osipov-Xiao-Rokhlin algorithm is more efficient and should be preferred.

Knowledge of $\chi_n(\gamma)$ is required by the algorithm of [2] for the rapid evaluation of $Ps_n(z;\gamma)$. Moreover, its running time can be substantially accelerated when the values of

$$\frac{d\,\Psi S_n}{dz}(0;\gamma),\ \frac{d^2\,\Psi S_n}{dz^2}(0;\gamma) \text{ and } \frac{d^3\,\Psi S_n}{dz^3}(0;\gamma) \tag{46}$$

are known. The technique described here to construct an expansion of $\chi_\sigma(\gamma)$ was also used to construct expansions of the quantities (46). However, the method was so similar to the procedure used to construct the expansion of $\chi_\sigma(\gamma)$ that we omit the details.

We first describe the form of the expansion used to represent $\chi_\sigma(\gamma)$. Then, we describe the method used to construct it.

6.1. The mechanism used to represent $\chi_\sigma(\gamma)$

A k-term Chebyshev expansion on the interval $[a, b]$ is a sum of the form

$$f(x) = \sum_{j=0}^{k-1} a_j T_j\left(\frac{2}{b-a}x + \frac{a+b}{a-b}\right), \tag{47}$$

where T_j denotes the Chebyshev polynomial of degree j. It is well known that the coefficients in the expansion (47) can be evaluated in a numerically stable fashion given its values at the k points

$$\frac{b+a}{2} - \frac{b-a}{2}\cos\left(\frac{j}{k}\pi\right), \quad j = 0, \ldots, k-1. \tag{48}$$

The set (48) is known as the k-point Chebyshev extrema grid on the interval $[a, b]$. Moreover, the barycentric Lagrange formula can be used to evaluate (47) in a numerically stable fashion at any point in $[a, b]$ given its values at the points (48). See, for instance, [18] for a thorough discussion of Chebyshev interpolation.

A piecewise k-term Chebyshev expansion comprises a partition

$$a = x_0 < x_1 < x_2 < \ldots < x_n = b \tag{49}$$

together with a collection of k-term Chebyshev expansions, one for each of the subintervals $[x_j, x_{j+1}]$. As with Chebyshev expansions, a piecewise Chebyshev expansion can be evaluated in a numerically stable fashion given either the coefficients in each of these expansions, or the values of each expansion at the nodes of the k-point Chebyshev extrema grid on the corresponding interval.

For each $l = 1, \ldots, 7$ we use I_l to denote the interval

$$I_l = \left[4^{2+l}, 4^{3+l}\right]. \tag{50}$$

Moreover, for each $l = 1, \ldots, 7$, we let

$$\gamma_0^{(l)}, \ldots, \gamma_{k-1}^{(l)} \tag{51}$$

be the nodes of the k-point Chebyshev extrema grid on the interval I_l, where $k = 30$. For each $l = 1, \ldots, 7$ and each $i = 0, \ldots, (k-1)$ we use a piecewise Chebyshev expansion on the interval

$(0, 1.1)$ to represent the function

$$f_i^{(l)}(\sigma) = \chi_\sigma\left(\gamma_i^{(l)}\right). \tag{52}$$

The number of terms in each of these Chebyshev expansions is $k = 30$, but the associated partitions of $(0, 1.1)$ vary. We found experimentally that the intervals I_l were a suitable partition of the domain of γ. The partitions for the piecewise Chebyshev expansions of the functions (52) were determined via an adaptive algorithm which is described in the next subsection.

Using the piecewise Chebyshev expansions of the functions (52), $\chi_\sigma(\gamma)$ can be evaluated for all $64 = 2^6 \leqslant \gamma \leqslant 2^{20} = 1,048,576$ and all $0 \leqslant \sigma \leqslant 1.1\gamma$. More explicitly, given a pair of parameters γ and σ at which we wish to evaluate the expansion, we first find an interval I_l containing γ (γ might be on the boundary between two of the subintervals, in which case either subinterval will serve). Next we evaluate

$$\chi_\sigma\left(\gamma_0^{(l)}\right), \ldots, \chi_\sigma\left(\gamma_{k-1}^{(l)}\right) \tag{53}$$

using the piecewise Chebyshev expansions of the functions (52). Finally, we use the barycentric Lagrange interpolation formula for the Chebyshev polynomials to evaluate $\chi_\sigma(\gamma)$ using the values (53).

6.2. Construction of the expansion

In [2], an algorithm for calculating the phase function $\Psi S_\chi(z;\gamma)$ for given values of the parameters γ and χ is described. Here, we detail how it can be used to construct a piecewise polynomial expansion of the function

$$f(\sigma) = \chi_\sigma(\gamma) \tag{54}$$

over the interval $0 \leqslant \sigma \leqslant 1.1$ for a fixed value of γ. This technique is, of course, applied with γ taking on each of the values

$$\gamma_i^{(l)}, \quad l = 1, \ldots, 7, , i = 0, \ldots, 29.$$

in order to construct the piecewise polynomial expansions of the functions (52).

As a first step, we calculate the value $\tilde{\chi}_1$ of the parameter χ corresponding to the characteristic exponent 0 and the value $\tilde{\chi}_2$ of the parameter χ corresponding to the characteristic exponent $m = \lceil 1.1\gamma \rceil$ using the Osipov-Xiao-Rokhlin method. Next, we construct a k-term piecewise Chebyshev expansion — with k again taken to be 30 — which represents the function

$$g(\chi) = -\frac{2}{\pi}\Psi S_\chi(0;\gamma) - 1 \tag{55}$$

over the interval $[\tilde{\chi}_1, \tilde{\chi}_2]$. We do this via an adaptive algorithm which operates as follows. It maintains two lists of intervals, one a list of processed intervals and the other a list of intervals to process. Initially, the interval $[\tilde{\chi}_1, \tilde{\chi}_2]$ is in the list of intervals to process and the list of processed intervals is empty. As long as the list of intervals to process is not empty, the following procedure is repeated:

1. Remove an interval $[a, b]$ from the list of intervals to process.
2. Use the algorithm of [2] to evaluate the function $g(\chi)$ at each of the nodes in the k-point Chebyshev extrema grid on $[a, b]$.

3. Compute the coefficients $a_0, \ldots, a_{k-1}$ in the Chebyshev expansion

$$\sum_{j=0}^{k-1} a_j T_j \left(\frac{2}{b-a} x + \frac{a+b}{a-b} \right)$$

which is equal to $g(\chi)$ at each of the nodes in the k-point Chebyshev extrema grid on $[a, b]$.

4. If

$$\sum_{j=k/2}^{k-1} a_j^2 < 100 \; \epsilon_0^2 \sum_{j=0}^{k-1} a_j^2,$$

where ϵ_0 is machine zero, then move the interval $[a, b]$ into the list of processed intervals. Otherwise, add the intervals $[a, (a+b)/2]$ and $[(a+b)/2, b]$ to the list of intervals to process.

When the process terminates, the list of processed intervals determines the partition of $[\tilde{\chi}_1, \tilde{\chi}_2]$ used by the piecewise Chebyshev expansion of $g(\chi)$.

The next step consists of constructing a piecewise Chebyshev expansion for the inverse function $f(\sigma)$ of $g(\chi)$. This is accomplished via an algorithm which is quite similar to that used to construct the expansion of $g(\chi)$. It also maintains a list of intervals to be processed and a list of processed intervals. Initially, $[0, 1.1]$ is placed in the list of intervals to process and the list of processed intervals is empty. The algorithm then repeats the following steps until the list of intervals to process is empty:

1. Remove an interval $[c, d]$ from the list of intervals to process.

2. Find α and β such that $g(\alpha) \leqslant c < d \leqslant g(\beta)$. The existence of α and β with these properties follows from the choice of the interval $[\tilde{\chi}_1, \tilde{\chi}_2]$ over which we represent the function g. Moreover, α and β can be found by examining the values of $g(\chi)$ at the nodes of the k-point Chebyshev grids on each of the subintervals associated with the piecewise Chebyshev expansion of g.

3. For each node σ_j in the k-point Chebyshev extrema grid on the interval $[a, b]$ compute the value of χ_j such that $g(\chi_j) = \sigma_j$ via bisection. Of course, we will also have $f(\sigma_j) = \chi_j$.

   More explicitly, we repeat the following steps until the quantity $|\alpha - \beta| / |\alpha|$ falls below $10\epsilon_0$:

   - Use the piecewise Chebyshev expansion of $g(\chi)$ to compute $g\left(\frac{\alpha+\beta}{2}\right)$.
   - If $g\left(\frac{\alpha+\beta}{2}\right) < \sigma_j$, then let $\alpha = \frac{\alpha+\beta}{2}$.
   - Otherwise, let $\beta = \frac{\alpha+\beta}{2}$.

4. Form the coefficients $b_0, \ldots, b_{k-1}$ in the Chebyshev expansion

$$\sum_{j=0}^{k-1} b_j T_j \left(\frac{2}{d-c} x + \frac{c+d}{c-d} \right)$$

which, for each $j = 0, \ldots, k-1$, takes on the value χ_j at the point σ_j.

5. If

$$\sum_{j=k/2}^{k-1} b_j^2 < 100 \; \epsilon_0^2 \sum_{j=0}^{k-1} b_j^2,$$

where ϵ_0 is machine zero, then move the interval $[c, d]$ into the list of processed intervals. Otherwise, add the intervals $[c, (c + d)/2]$ and $[(c + d)/2, d]$ to the list of intervals to process.

The list of processed intervals determines the partition of $[0, 1.1]$ used by the piecewise Chebyshev expansion of the inverse function $f(\sigma)$ of $g(\chi)$.

7. Numerical experiments

In this section, we present the results of numerical experiments which were conducted to to illustrate the effectiveness of the algorithm of this article. The code for these experiments was written in Fortran and compiled with version 11.1.0 of the the GNU Fortran compiler. They were performed on a desktop computer equipped with an AMD Ryzen 3900X processor. An implementation of our algorithm and code for conducting all of the experiments discussed here is available on GitHub at the following address:

`https://github.com/JamesCBremerJr/Prolates`

The expansion of $\chi_\sigma(\gamma)$ used in these experiments allows us to evaluate it over the following ranges of the parameters:

$$2^6 \leqslant \gamma \leqslant 2^{20} \quad \text{and} \quad 0 \leqslant \sigma \leqslant 1.1.$$

It occupies less than 0.76 megabytes of memory.

In some of these experiments, we compared the performance of our algorithm with that of the Osipov-Xiao-Rokhlin method [14]. Its running time is highly dependent on the dimension of the tridiagonal matrix formed in order to calculate $\chi_n(\gamma)$. Most implementations use a highly conservative value for this dimension. The authors of [14], for instance, take it to be $1000 + n + \lfloor 1.1\gamma \rfloor$ in their implementation. The experiments of [16], however, suggest that the necessary dimension grows as $\mathcal{O}\left(n + \sqrt{n\gamma}\right)$. It is difficult to find a simple formula which suffices in all cases of interest. Accordingly, our implementation of the Osipov-Rokhlin-Xiao algorithm initially takes the estimate to be

$$50 + \left\lfloor \frac{2}{\pi} n \right\rfloor + \lfloor \sqrt{\gamma n} \rfloor, \tag{56}$$

which we found to be sufficient for a large range of parameters, and then increases the dimension adaptively as needed to ensure high accuracy. Our implementation can be found in the GitHub repository mentioned above.

To account for the vagaries of modern computational environments, all times reported here were obtained by repeating each calculation 100 times and averaging the result.

7.1. The accuracy with which $\chi_n(\gamma)$ is calculated

In this first set of experiments, we measured the accuracy with which $\chi_\sigma(\gamma)$ is calculated for various ranges of values of the parameters. In each experiment, we fixed a range $[\gamma_1, \gamma_2]$ of values of γ and a range $[\sigma_1, \sigma_2]$ of values of σ. We sampled 100 random values of γ in $[\gamma_1, \gamma_2]$ and 100 random integers n in the interval $[\gamma\sigma_1, \gamma\sigma_2]$. For each of the $10,000$ pairs of the sampled parameters, we calculated $\chi_n(\gamma)$ and compared the result with that obtained by running the Osipov-Xiao-Rokhlin algorithm using extended precision (Fortran REAL*10) arithmetic. Our algorithm was executed using double precision arithmetic. We used extended precision for the Osipov-Xiao-Rokhlin algorithm because it looses a few digits of accuracy for certain values of the parameters, mainly in cases in which γ is large and n is small. Table 1 reports the results. Each row there reports the maximum relative error in $\chi_n(\gamma)$ encountered for each range of values of the parameters considered.

Range of γ	Range of σ	Max relative error	Range of γ	Range of σ	Max relative error
4^3 to 4^4	$0.00 - 0.25$	4.95×10^{-15}	4^7 to 4^8	$0.00 - 0.25$	4.92×10^{-15}
	$0.25 - 0.50$	4.82×10^{-15}		$0.25 - 0.50$	3.91×10^{-15}
	$0.50 - 0.75$	5.61×10^{-15}		$0.50 - 0.75$	4.06×10^{-15}
	$0.75 - 1.00$	5.33×10^{-15}		$0.75 - 1.00$	4.38×10^{-15}
4^4 to 4^5	$0.00 - 0.25$	5.05×10^{-15}	4^8 to 4^9	$0.00 - 0.25$	5.12×10^{-15}
	$0.25 - 0.50$	4.03×10^{-15}		$0.25 - 0.50$	4.35×10^{-15}
	$0.50 - 0.75$	4.80×10^{-15}		$0.50 - 0.75$	4.18×10^{-15}
	$0.75 - 1.00$	5.11×10^{-15}		$0.75 - 1.00$	4.44×10^{-15}
4^5 to 4^6	$0.00 - 0.25$	4.85×10^{-15}	4^9 to 4^{10}	$0.00 - 0.25$	4.68×10^{-15}
	$0.25 - 0.50$	4.13×10^{-15}		$0.25 - 0.50$	3.82×10^{-15}
	$0.50 - 0.75$	4.27×10^{-15}		$0.50 - 0.75$	4.23×10^{-15}
	$0.75 - 1.00$	4.37×10^{-15}		$0.75 - 1.00$	4.42×10^{-15}
4^6 to 4^7	$0.00 - 0.25$	5.01×10^{-15}			
	$0.25 - 0.50$	3.63×10^{-15}			
	$0.50 - 0.75$	3.97×10^{-15}			
	$0.75 - 1.00$	4.48×10^{-15}			

Table 1: The maximum relative error encountered while evaluating $\chi_n(\gamma)$ for various ranges of the parameters.

7.2. The time with required to calculate $\chi_\sigma(\gamma)$

In the experiments described here, we measured the time required to evaluate $\chi_\sigma(\gamma)$ using the algorithm of this paper.

Table 2 reports the results of the first set of such experiments. In each experiment, we fixed a range $[\gamma_1, \gamma_2]$ of values of γ and a range $[\sigma_1, \sigma_2]$ of values of σ. We sampled 100 random values of γ in $[\gamma_1, \gamma_2]$ and 100 random integers n in the interval $[\sigma_1\gamma, \sigma_2\gamma]$. We then measured the time required to evaluate $\chi_n(\gamma)$ at each of the $10,000$ pairs of the sampled parameters using our algorithm and using the Osipov-Xiao-Rokhlin method. The average time required by each approach is reported in Table 2.

In a second set of experiments, we measured the time required to evaluate $\chi_\sigma(\gamma)$ as γ varies for certain fixed values of σ and the time required to evaluate $\chi_\sigma(\gamma)$ as σ varies for certain fixed values of γ. Figure 3 gives the results.

8. Acknowledgements

The second author was supported in part by an NSERC Discovery grant RGPIN-2021-02613, and by NSF grants DMS-1818820 and DMS-2012487.

Range of γ	Range of σ	Average Time expansion	Average time Rokhlin, et. al.
4^3 to 4^4	$0.00 - 0.25$	1.04×10^{-06}	5.28×10^{-05}
	$0.25 - 0.50$	1.09×10^{-06}	6.86×10^{-05}
	$0.50 - 0.75$	1.25×10^{-06}	8.40×10^{-05}
	$0.75 - 1.00$	1.41×10^{-06}	1.01×10^{-04}
4^4 to 4^5	$0.00 - 0.25$	1.08×10^{-06}	1.38×10^{-04}
	$0.25 - 0.50$	1.17×10^{-06}	2.16×10^{-04}
	$0.50 - 0.75$	1.38×10^{-06}	2.97×10^{-04}
	$0.75 - 1.00$	1.59×10^{-06}	3.64×10^{-04}
4^5 to 4^6	$0.00 - 0.25$	1.18×10^{-06}	4.17×10^{-04}
	$0.25 - 0.50$	1.29×10^{-06}	8.30×10^{-04}
	$0.50 - 0.75$	1.49×10^{-06}	1.06×10^{-03}
	$0.75 - 1.00$	1.69×10^{-06}	1.41×10^{-03}
4^6 to 4^7	$0.00 - 0.25$	1.27×10^{-06}	1.62×10^{-03}
	$0.25 - 0.50$	1.34×10^{-06}	3.01×10^{-03}
	$0.50 - 0.75$	1.54×10^{-06}	4.26×10^{-03}
	$0.75 - 1.00$	1.76×10^{-06}	5.29×10^{-03}
4^7 to 4^8	$0.00 - 0.25$	1.33×10^{-06}	6.40×10^{-03}
	$0.25 - 0.50$	1.36×10^{-06}	1.21×10^{-02}
	$0.50 - 0.75$	1.61×10^{-06}	1.73×10^{-02}
	$0.75 - 1.00$	1.86×10^{-06}	2.13×10^{-02}
4^8 to 4^9	$0.00 - 0.25$	1.46×10^{-06}	2.50×10^{-02}
	$0.25 - 0.50$	1.49×10^{-06}	4.60×10^{-02}
	$0.50 - 0.75$	1.77×10^{-06}	6.73×10^{-02}
	$0.75 - 1.00$	1.98×10^{-06}	7.56×10^{-02}
4^9 to 4^{10}	$0.00 - 0.25$	1.58×10^{-06}	9.86×10^{-02}
	$0.25 - 0.50$	1.59×10^{-06}	1.86×10^{-01}
	$0.50 - 0.75$	1.82×10^{-06}	2.81×10^{-01}
	$0.75 - 1.00$	2.04×10^{-06}	3.22×10^{-01}

Table 2: The average time (in seconds) required to evaluate $\chi_n(\gamma)$ using the algorithm of this paper and the Osipov-Xiao-Rokhlin algorithm for various ranges of the parameters.

References

[1] Amos, D. E. Algorithm 644: a portable package for Bessel functions of a complex argument and nonnegative order. *ACM Transactions on Mathematica Software 3* (1986), 265–273.

[2] Bremer, J. On the numerical evaluation of the prolate spheroidal wave functions of order zero.

[3] Durand, L. Product formulas and Nicholson-type integrals for Jacobi functions. I: Summary of results. *Siam Journal on Mathematical Analysis 9* (1978), 76–86.

[4] Goldstein, M., and Thaler, R. M. Bessel functions for large arguments. *Mathematical Tables and Other Aids to Computation 12* (1958), 18–26.

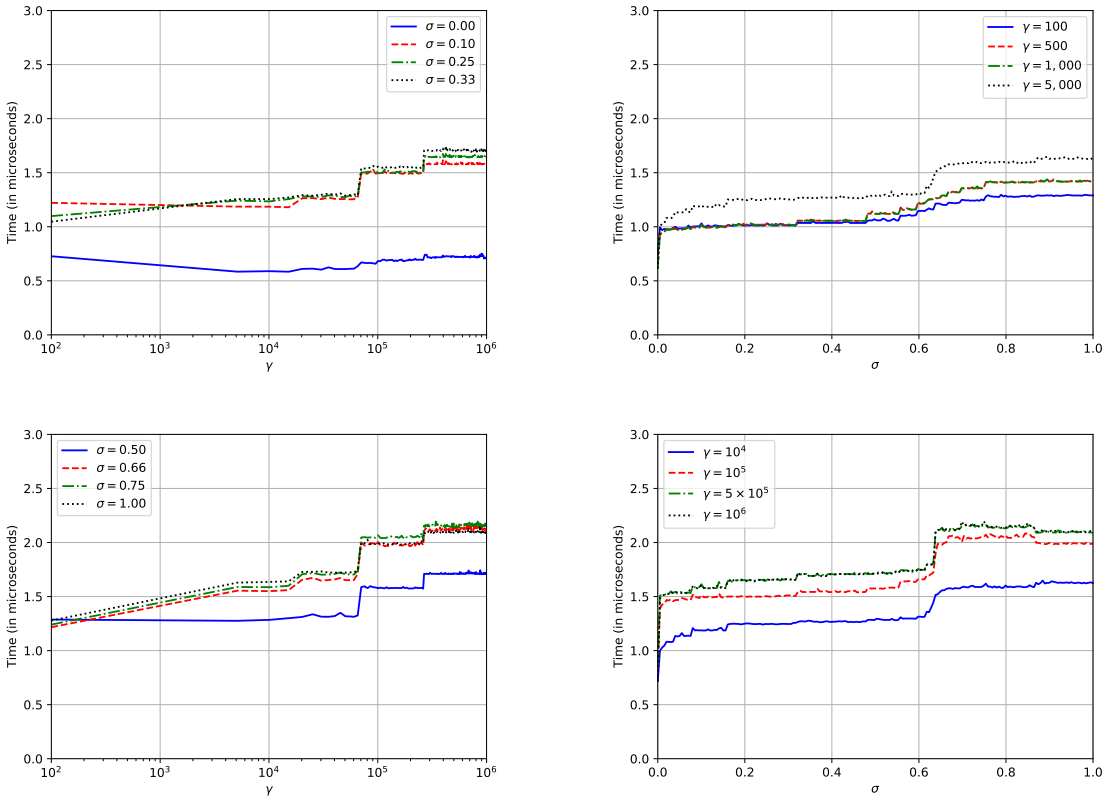

Figure 3: The time (in microseconds) required by the algorithm of this article to evaluate $\chi_\sigma(\gamma)$. Each plot on the left gives the time as a function of γ for various values of σ, and each plot on the right gives the time as a function of σ for various values of γ. A logarithmic scale is used for the x-axis in each of the graphs on the left.

[5] Hartman, P. On differential equations and the function $J_\mu^2 + Y_\mu^2$. *American Journal of Mathemtics 83* (1961), 154–188.

[6] Hartman, P. On differential equations, Volterra equations and the function $J_\mu^2 + Y_\mu^2$. *American Journal of Mathemtics 95* (1973), 553–593.

[7] Hille, E. *Ordinary Differential Equations in the Complex Plane*. John Wiley and Sons, 1976.

[8] Imam, M. *Studies in the associated Mathieu equation and the spheroidal wave equation*. PhD thesis, University of Surrey, 1967. Available at `http://epubs.surrey.ac.uk/id/eprint/848153`.

[9] Ince, E. *Ordinary Differential Equations*. Dover, 1956.

[10] Kummer, E. De generali quadam aequatione differentiali tertti ordinis. *Progr. Evang. Köngil. Stadtgymnasium Liegnitz* (1834).

[11] Landau, H. J., and Widom, H. Eigenvalue distribution of time and frequency limiting. *Journal of Mathematical Analysis and Applications 77* (1980), 469–481.

[12] Meixner, J., and Schäfke, F. *Mathieusche Funktionen und Sphäroidfunktionen*. Springer-Verlag, 1954 (in German).

[13] Morse, P. M., and Feshbach, H. *Methods of Mathematical Physics, Part I.* Feshbach Publishing, 1998.

[14] Osipov, A., Rokhlin, V., and Xiao, H. *Prolate Spheroidal Wave Functions of Order* 0. Springer, 2013.

[15] Rehan, R., and Bremer, J. An $\mathcal{O}(1)$ algorithm for the numerical evaluation of the Sturm-Liouville eigenvalues of the spheroidal wave functions of order zero.

[16] Schmutzhard, S., Hrycak, T., and Feichtinger, H. A numerical study of the Legendre-Galerkin method for the evaluation of the prolate spheroidal wave functions. *Numerical Algorithms 68* (2015), 1017–1398.

[17] Slepian, D., and Pollak, H. Prolate spheroidal wave functions, Fourier analysis and uncertainty — I. *The Bell System Technical Journal 40* (1961), 43–64.

[18] Trefethen, N. *Approximation Theory and Approximation Practice.* Society for Industrial and Applied Mathematics, Philadelphia, PA, 2013.

[19] Widder, D. *The Laplace Transform.* Princeton University Press, 1946.

[20] Williamson, R. Multiply monotone functions and their Laplace transforms. *Duke Math Journal 23* (1956), 189–207.

[21] Xiao, H., Rokhlin, V., and Yarvin, N. Prolate spheroidal wavefunctions, quadrature and interpolation. *Inverse Problems 17* (2001), 805–838.

[22] Zettl, A. *Sturm-Liouville Theory.* American Mathematical Society, 2005.